

SCIENTIFIC REPORTS



Corrected: Author Correction

OPEN

A comprehensive bioinformatics analysis on multiple Gene Expression Omnibus datasets of nonalcoholic fatty liver disease and nonalcoholic steatohepatitis

Shanzhou Huang^{1,2,3}, Chengjun Sun^{1,2,3}, Yuchen Hou^{1,2,3}, Yunhua Tang^{1,2,3}, Zebin Zhu^{1,2,3}, Zhiheng Zhang^{1,2,3}, Yixi Zhang^{1,2,3}, Linhe Wang^{1,2,3}, Qiang Zhao^{1,2,3}, Mao-Gen Chen^{1,2,3}, Zhiyong Guo^{1,2,3}, Dongping Wang^{1,2,3}, Weiqiang Ju^{1,2,3}, Qi Zhou⁴, Linwei Wu^{1,2,3} & Xiaoshun He^{1,2,3}

Fatty liver disease is one of the leading causes of chronic damage in western countries. Approximately 25% of adults in the United States have fatty livers in the absence of excessive alcohol consumption, a condition termed nonalcoholic fatty liver disease (NAFLD). Little is known about the prevalence and genetic background of NAFLD or the factors that determine its development. In this study, we used the Gene-Cloud of Biotechnology Information bioinformatics platform to carry out a comprehensive bioinformatics analysis identifying differentially expressed genes (DEGs), key biological processes and intersecting pathways. We imported 3 Gene Expression Omnibus datasets (GSE66676, GSE49541, and GSE834521). Then, we assessed the expression of the DEGs in clinical samples. We found that CD24 was the only gene co-expressed in all 3 datasets. "Glycolysis/gluconeogenesis", "p53 signaling pathway" and "glycine, serine and threonine metabolism" were 3 common pathways related to the fatty liver process. In NAFLD tissues, CD24, COL1A1, LUM, THBS2 and EPHA3 were upregulated, and PZP was downregulated. CD24 is a core gene among these DEGs and have not yet been studied of its impact on NAFLD. Co-expressed genes, common biological processes and intersecting pathways identified in the study might play an important role in NAFLD progression. Further studies are needed to elucidate the mechanism of these potential genes and pathways in NAFLD.

Nonalcoholic fatty liver disease (NAFLD) and its subtype nonalcoholic steatohepatitis (NASH) have become an increasingly important clinical and economic burden for public health^{1,2}. NAFLD is the leading cause of liver damage and dysfunction in the western world and is strongly associated with obesity and insulin resistance³. Fatty liver could subsequently develop to malignancy and end-stage liver failure⁴⁻⁶. Currently, NAFLD is a leading indication for liver transplantation in the United States⁷. Mechanistic, preclinical, and clinical studies provided an initial view into NAFLD progression along with the process from NAFLD to NASH and fibrosis^{8,9}. However, owing to the epidemics of NAFLD and the unclear mechanism of NAFLD progression, it is important to elucidate the underlying NAFLD mechanisms in detail.

Gene profiling experiments in cross-sectional studies have been useful in identifying factors involved in NAFLD progression¹⁰⁻¹². Gene profiling studies identified novel targets of NAFLD and demonstrated the roles of specific metabolic and repair pathways in the disease¹¹. In the present study, we carried out a comprehensive bioinformatics analysis between normal liver tissues and NAFLD/NASH tissues on the Gene-Cloud of

¹Organ Transplant Center, The First Affiliated Hospital, Sun Yat-sen University, Guangzhou, 510080, China.

²Guangdong Provincial Key Laboratory of Organ Donation and Transplant Immunology, Guangzhou, 510080, China. ³Guangdong Provincial International Cooperation Base of Science and Technology (Organ Transplantation), Guangzhou, 510080, China. ⁴Department of General Surgery, Hui Ya Hospital of The First Affiliated Hospital, Sun Yat-sen University, Huizhou, Guangdong, 516081, China. Shanzhou Huang, Chengjun Sun and Yuchen Hou contributed equally to this work. Correspondence and requests for materials should be addressed to Q. Zhou (email: hnzhouqi@163.com) or L. Wu (email: lw97002@163.com) or X.H. (email: gdtcr@163.com)

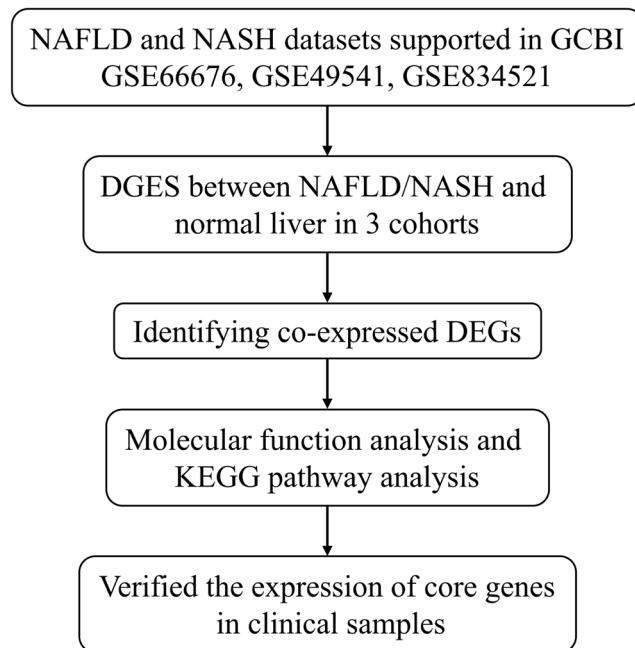


Figure 1. Flow diagram of the study design. NAFLD, nonalcoholic fatty liver disease; NASH, nonalcoholic steatohepatitis; DEGs, differentially expressed genes; KEGG, Kyoto Encyclopedia of Genes and Genomes.

Biotechnology Information (GCBI) bioinformatics platform. Based on the comprehensive bioinformatics analysis, we determined to identify key differentially expressed genes (DEGs), biological processes and pathways that are closely associated with NAFLD/NASH.

Materials and Methods

Gene expression omnibus datasets. The Gene Expression Omnibus (GEO) (<https://www.ncbi.nlm.nih.gov/gds>) is a public repository at the National Center of Biotechnology Information for storing high-throughput gene expression datasets. We selected potential GEO datasets according to the following inclusion criteria: 1) specimens had histological diagnosis; 2) human liver tissues diagnosed as hepatocyte steatosis for the experimental group; 3) normal liver tissues used as controls; 4) expression profiling by array and raw data had the CEL format; 5) performed on the GPL570 platform ([HGU133_Plus_2] Affymetrix Human Genome U133 Plus 2.0 Array) and Human Exon 1.0 ST v1 Array; and 6) supported by GCBI analysis laboratory. Datasets with specimens from other organisms, expression profiling by RT-PCR (or genome variation profiling by SNP array/SNP genotyping by SNP array), analyses on platforms other than GPL570, or sample size <10 were excluded.

We used the search terms “Fatty liver” [MeSH Terms] AND “Homo sapiens” [Organism] and “Non-alcoholic” [Description] and “CEL” [Supplementary Files] and “Expression profiling by array” [DataSet Type] in the GEO DataSets to identify potential datasets. Then, we further screened these datasets according to the above inclusion criteria. Finally, 3 GEO datasets, GSE66676, GSE49541, and GSE834521, were included in our study.

Gene-Cloud of Biotechnology Information (GCBI). GCBI (Shanghai, China, <https://www.gcbi.com.cn>) is an online comprehensive bioinformatics analysis platform that combines a variety of research findings, genetic information, sample information, data algorithms and bioinformatics to create a “gene knowledge base,” which involves GEO datasets. GCBI platform can systematically analyze GEO dataset-derived gene expression information¹³, including more than 120 million copies of genomic samples. In the present study, GCBI was used to identify DEGs between NAFLD/NASH liver tissues and normal liver tissues. In the Differential Gene Expression Analysis module on the GCBI platform, we identified DEGs with a fold expression change >5 at cut off values $Q < 0.05$ and $P < 0.05$. Venn diagrams were used to compare the top 100 DEGs from 3 cohorts by Venny (<http://bioinfopnp.cnb.csic.es/tools/venny/index.html>). Based on the DEGs, we further performed gene ontology (GO) analysis in terms of biological functions and Kyoto Encyclopedia of Genes and Genomes (KEGG) analysis in terms of pathway analysis. The top 20 biological functions and pathways are presented. Furthermore, a pathway relation network module was used to identify the core networks and pathway connections. Then, we applied the Gene Co-expression Network module on the GCBI platform to build gene co-expression networks for the DEGs to determine core genes in the networks.

Tissue specimens, RNA extraction and qRT-PCR analysis. 15 healthy liver tissues and 10 fatty liver tissues from liver donors were enrolled in our study to validate the expression levels of co-expressed DEGs. Prior patient consent and ethical approval from the ethics committee of the First Affiliated Hospital, Sun Yat-sen were obtained. All methods were performed in accordance with the ethics guidelines and regulations. We selected 8

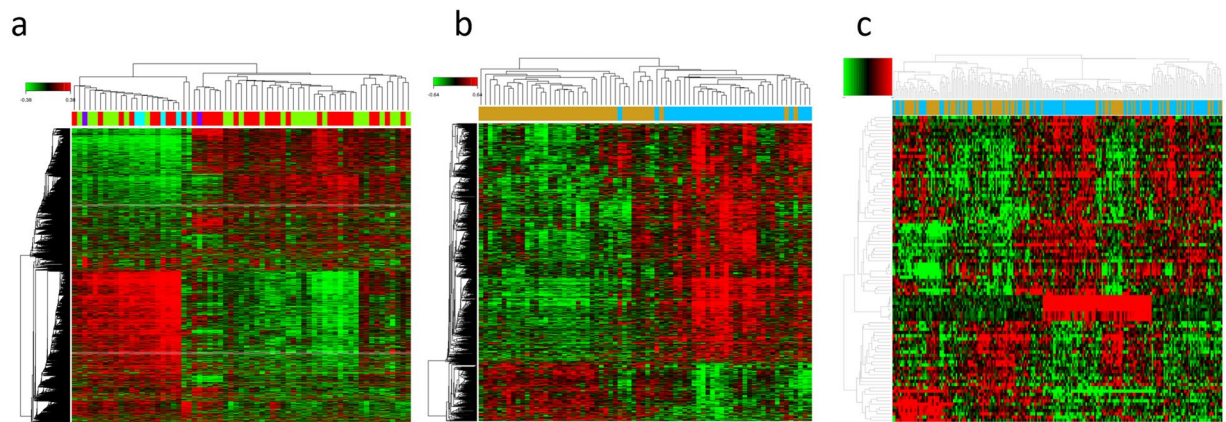


Figure 2. (a–c) Heat maps for potential DEGs between fatty liver and normal liver tissues in 3 cohorts. Heat maps for potential DEGs in GSE66676 (containing 33 NAFLD/NASH tissues and 34 normal liver tissues) (a), GSE49541 (containing contained 32 advanced NAFLD tissues and 40 mild NAFLD tissues) (b), and GSE834521 (126 NASH tissues and 98 normal liver tissues) (c).

Rank	Probe Set ID	Gene Symbol	Gene Description	Regulation
1	7903765	GSTM1	glutathione S-transferase mu 1	Downregulated
2	8096301	SPP1	secreted phosphoprotein 1	Upregulated
3	8151532	FABP4	fatty acid binding protein 4	Upregulated
4	7960984	PZP	pregnancy-zone protein	Downregulated
5	7914000	NR0B2	nuclear receptor subfamily 0, group B, member 2	Downregulated
6	8174474	ACSL4	acyl-CoA synthetase long-chain family member 4	Upregulated
7	7908481	CFHR3	complement factor H-related 3	Upregulated
8	8136336	AKR1B10	aldo-keto reductase family 1, member B10	Upregulated
9	8150920	CYP7A1	cytochrome P450, family 7, subfamily A, polypeptide 1	Upregulated
10	7948420	FABP5	fatty acid binding protein 5	Upregulated

Table 1. Top 10 differentially expressed genes in Cohort 1.

Rank	Probe Set ID	Gene Symbol	Gene Description	Regulation
1	201842_s_at	EFEMP1	EGF containing fibulin-like extracellular matrix protein 1	Upregulation
2	201843_s_at	EFEMP1	EGF containing fibulin-like extracellular matrix protein 1	Upregulation
3	205422_s_at	ITGBL1	integrin, beta-like 1	Upregulation
4	201744_s_at	LUM	lumican	Upregulation
5	214247_s_at	DKK3	dickkopf WNT signaling pathway inhibitor 3	Upregulation
6	213071_at	DPT	dermatopontin	Upregulation
7	1557080_s_at	ITGBL1	integrin, beta-like 1 (with EGF-like repeat domains)	Upregulation
8	206070_s_at	EPHA3	EPH receptor A3	Upregulation
9	207173_x_at	CDH11	cadherin 11, type 2, OB-cadherin	Upregulation
10	209291_at	ID4	inhibitor of DNA binding 4	Upregulation

Table 2. Top 10 differentially expressed genes in Cohort 2.

co-expressed DEGs, including CD24, PZP, COL1A1, COL1A2, LUM, VCAN, THBS2 and EPHA3, for validation. All tissues were histologically diagnosed. Total RNA from the tissue specimens was isolated using TRIzol reagent (Invitrogen, Carlsbad, California, USA), and qRT-PCR was performed with SYBR[®] Green dye (TaKaRa, Shiga, Japan), following the manufacturer's instructions. The primer sequences are provided in Supplementary Table S1. β -tubulin was used as a reference gene.

Ethics statement. The research protocol was reviewed and approved by the Research Ethics Committee of the First Affiliated Hospital, Sun Yat-sen. All experiments were conducted in accordance with approved guidelines of the First Affiliated Hospital, Sun Yat-sen University.

Rank	Probe Set ID	Gene Symbol	Gene Description	Regulation
1	16829985	ENO3	enolase 3 (beta, muscle)	Upregulation
2	16766132	APOF	apolipoprotein F	Downregulation
3	16895179	TP53I3	tumor protein p53 inducible protein 3	Upregulation
4	17104259	MSN	moesin (MSN)	Upregulation
5	16789484	ADSSL1	adenylosuccinate synthase like 1 (ADSSL1)	Upregulation
6	16977052	CXCL10	chemokine (C-X-C motif) ligand 10	Upregulation
7	16890891	VIL1	villin 1	Downregulation
8	16909401	SLC16A14	solute carrier family 16, member 14	Upregulation
9	16811975	TSPAN3	tetraspanin 3	Upregulation
10	16841768	CENPV	centromere protein V	Downregulation

Table 3. Top 10 differentially expressed genes in Cohort 3.

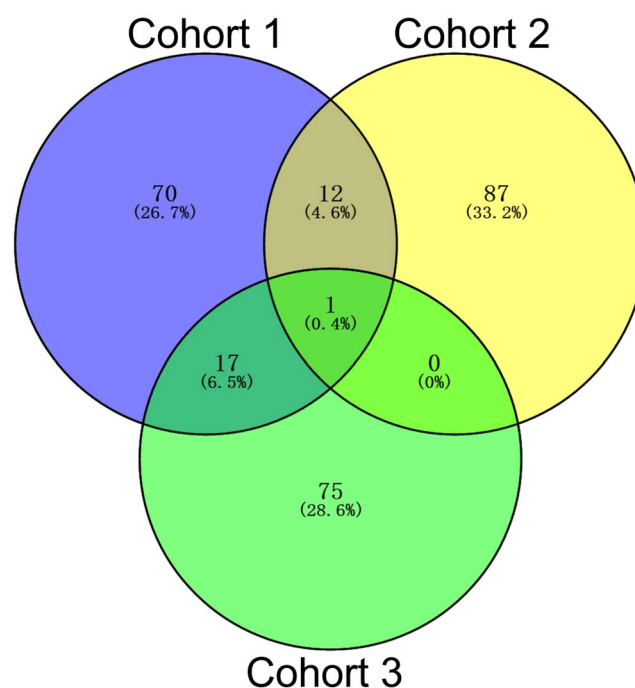


Figure 3. The Venn diagram shows the top 100 DEGs and co-expressed genes among cohort 1 (GSE66676), cohort 2 (GSE49541) and cohort 3 (GSE834521).

Ethical approval. All procedures performed in studies involving human participants were in accordance with the ethical standards of the ethical committee of the First Affiliated Hospital, Sun Yat-sen University were obtained and with the 1964 Helsinki Declaration and its later amendments or comparable. NO tissues were procured from prisoners. All the livers were procured in Organ Transplant Center, The First Affiliated Hospital, Sun Yat-sen University.

Ethical standards. Informed consent was obtained from all individual participants included in the study.

Statistical analysis. Data are presented as the mean \pm SD for continuous variables. Student's t-test and analysis of variance were used to evaluate significant differences in demographic data. All P values were two-sided, and $P < 0.05$ was defined as statistically significant. Analyses were carried out by the Statistical Package for the Social Science (SPSS) 22.0 (IBM, USA).

Results

Study design. The flow diagram of our study design is shown in Fig. 1. Our initial aim was to identify core genes in the development of fatty liver. We used 3 GEO datasets (GSE66676, GSE49541, and GSE834521) in the GCBI bioinformatics analysis platform. We extracted gene expression data of NAFLD/NASH and normal liver tissues to identify DEGs between the two histological diagnosis types in these 3 cohorts. Co-expressed DEGs were identified based on these DEGs. Biological function and KEGG pathway analyses were then performed. Finally, we verified expression of the core co-expressed genes in clinical samples to confirm the results.

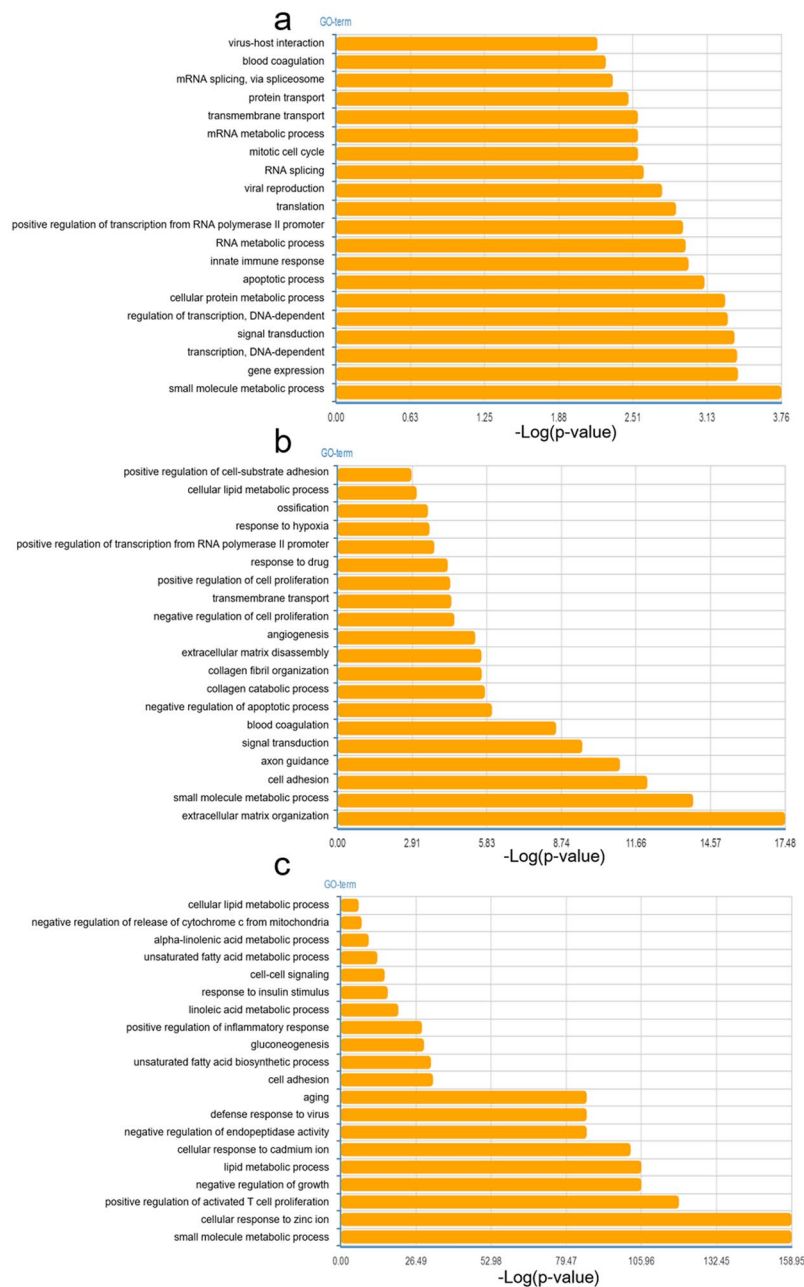


Figure 4. (a–c) Top 20 biological functions in terms of GO analysis related to DEGs in cohort 1 (a), cohort 2 (b) and cohort 3 (c).

Major characteristics of samples in 3 datasets. GEO datasets GSE66676 (Cohort 1), GSE49541 (Cohort 2), and GSE834521 (Cohort 3) were enrolled in our study. All 3 datasets were available in the GCBI bioinformatics analysis platform. GSE66676 contained 33 NAFLD or NASH tissues and 34 normal liver tissues. GSE49541 contained 32 advanced NAFLD tissues and 40 mild NAFLD tissues. GSE834521 included 126 NASH tissues and 98 normal liver tissues.

DEGs between NAFLD/NASH and normal liver tissues. We identified 8503, 1538, and 94 potential DEGs in GSE66676, GSE49541, and GSE834521, respectively (Fig. 2a–c). The top 10 DEGs from 3 cohorts are shown in Tables 1–3. After removing duplicate genes and expression values lacking specific gene symbols, we used the top 100 DEGs from GSE66676 and GSE49541 and 93 DEGs from GSE834521 to create a Venn diagram. The intersection of these 3 datasets in Fig. 3 shows that CD24 was the only co-expressed DEG found in all 3 cohorts. Twelve genes were co-expressed in Cohort 1 and Cohort 2, including COL1A1, COL1A2, MOXD1, LUM, VCAN, EFEMP1, THBS2, MGP, COL3A1, EPHA3, BICC1, and COL6A3, all of which were upregulated. Seventeen genes were co-expressed in Cohort 1 and Cohort 3, including SPP1, FABP4, PZP, UTY, SLC1A2, GPNMB, DDX3Y, SAA1, MT1M, FAT1, USP9Y, LYZ, CXCL10, VIL1, EIF1AY, UBD, and CYP3A43. Further

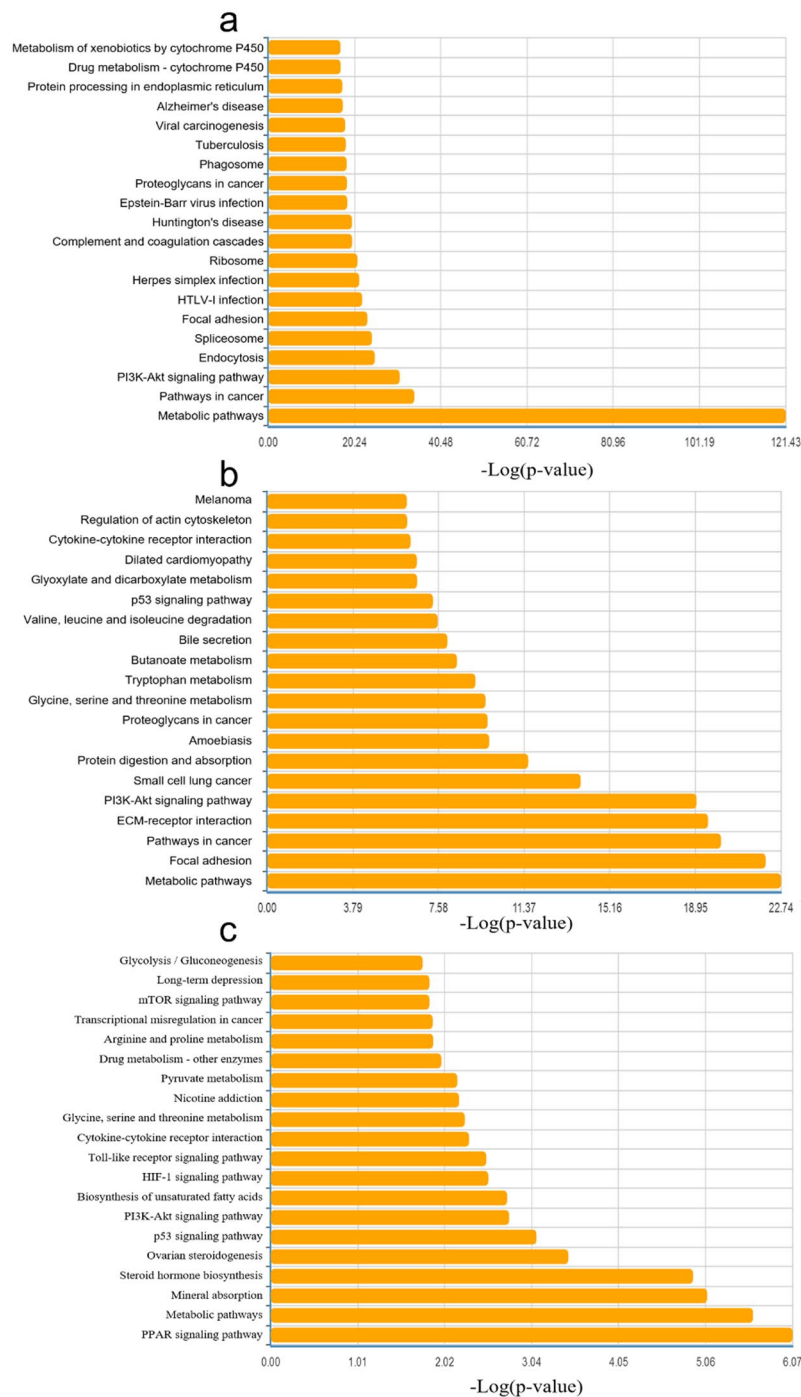


Figure 5. (a–c) Top 20 pathways in terms of KEGG pathway analysis related to DEGs in cohort 1 (a), cohort 2 (b) and cohort 3 (c). (d–f) Pathway relation network in 3 cohorts.

investigation showed that the regulation of MT1M, SLC1A2, CYP3A43 and VIL1 was not consistent. Therefore, 13 genes were co-expressed in Cohort 1 and Cohort 3.

Biological process analysis. In the present study, GO analysis was applied to investigate the biological function of the DEGs. The biological process analysis (Fig. 4a–c) revealed that “small molecule metabolic process” was a common biological function in 3 cohorts. “Cellular lipid metabolic process” and “cell adhesion” were the common biological processes in Cohort 2 and Cohort 3. Four common biological processes in Cohort 1 and Cohort 2 were “blood coagulation, transmembrane transport, positive regulation of transcription from RNA polymerase II promoter and signal transduction”. Metabolic processes, such as “alpha-linolenic acid metabolic process, unsaturated fatty acid metabolic process, mRNA/RNA metabolic process” and other biological processes, were also vital in each cohort.

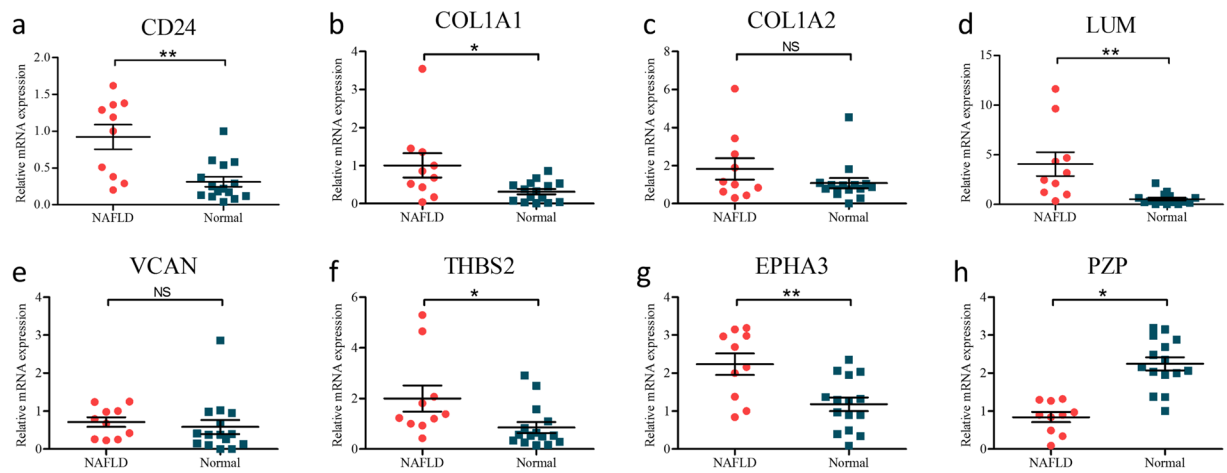


Figure 6. (a–h) Real-time qPCR validation of 8 co-expressed DEGs in 10 NAFLD and 15 normal liver tissues. * $P < 0.05$, ** $P < 0.01$, NS represents no significant difference, analysis by non-paired t tests.

Rank	Cohort 1	Cohort 2	Cohort 3
1	MAPK signaling pathway	MAPK signaling pathway	Pyruvate metabolism
2	Apoptosis	Pathways in cancer	Glycolysis/Gluconeogenesis
3	Pathways in cancer	Apoptosis	Fatty acid biosynthesis
4	Cell cycle	Cell cycle	Glycine, serine and threonine metabolism
5	Glycolysis/Gluconeogenesis	p53 signaling pathway	Prostate cancer
6	p53 signaling pathway	Pyruvate metabolism	Cytokine-cytokine receptor interaction
7	Glycine, serine and threonine metabolism	Glycolysis/Gluconeogenesis	Toll-like receptor signaling pathway
8	Calcium signaling pathway	Wnt signaling pathway	p53 signaling pathway
9	Citrate cycle (TCA cycle)	Focal adhesion	
10	Wnt signaling pathway	Glycine, serine and threonine metabolism	

Table 4. Top 10 pathways in pathway relation network of the 3 cohorts.

Pathway analysis. KEGG pathway analysis were used to investigate the pathway based on the DEGs identified. Figure 5a–c shows the top 20 pathways involved in each cohort. Among them, glycine, serine and threonine metabolism; cytokine-cytokine receptor interaction; PI3K-Akt signaling pathway; p53 signaling pathway; and metabolic pathways were 5 common pathways related to the fatty liver process. Among the top ten pathways in the pathway relation network in 3 cohorts, “glycolysis/gluconeogenesis”, “p53 signaling pathway” and “glycine, serine and threonine metabolism” were 3 intersecting pathways in the relation network (Table 4). MAPK signaling pathway, apoptosis, pathways in cancer, cell cycle, Wnt signaling pathway and pyruvate metabolism were the other intersecting pathways in pairwise comparisons.

The validation of core genes expression in clinical samples. To further determine which genes might play a significant role in the progression of fatty liver, we used real-time qPCR to detect the expression of 8 DEGs using clinical samples, including CD24, PZP, COL1A1, COL1A2, LUM, VCAN, THBS2 and EPHA3. 15 healthy liver tissues and 10 fatty liver tissues from liver donors were enrolled. We noted that CD24, COL1A1, LUM, THBS2 and EPHA3 were usually upregulated in fatty liver tissues comparing to normal liver tissues, which is consistent with the results of bioinformatics analysis above (Fig. 6a–f). PZP was significantly downregulated in fatty livers compared with normal livers, which is also consistent with the co-expressed results (Fig. 6h).

Discussion

Non-alcoholic steatohepatitis is strongly associated with strong genetic component and dietary component¹. A number of genes could be associated with the susceptibility and development of NAFLD and NASH^{1,2}. In our present study, we imported three GEO datasets into the GCBI comprehensive analysis platform to extract gene expression data of NAFLD/NASH tissue comparing to normal liver tissue or NASH tissue comparing to NAFLD liver tissue. We identified co-expressed DEGs, common biological processes and pathways between NAFLD/NASH and normal liver tissues through differential expression analysis in GCBI.

We found that CD24, PZP, COL1A1, COL1A2, LUM, VCAN, THBS2 and EPHA3 were potential biomarkers for distinguishing NAFLD/NASH. Further validation by clinical samples, the expression of CD24, PZP, COL1A1, LUM, THBS2 and EPHA3 were significantly regulated. Moreover, CD24 is a core gene among these DEGs and have not yet been studied of its impact on hepatocyte steatosis. CD24 encodes a sialoglycoprotein that is expressed on mature granulocytes and B cells and modulates growth and differentiation signals to these cells¹³. Several

studies have reported that CD24 is widely distributed, including on hematopoietic cells¹⁴ and non-hematopoietic cells^{15,16}. CD24 has been studied to be associated with various pathophysiological processes, including tracking divergent states of cells¹⁷, regulating CD8 (+) T cell activation¹⁸ and participating in mutant-IDH1-dependent chromatin state reprogramming¹⁹. Accumulating evidence showed that this protein is overexpressed in many types of cancers, resulting in cancer cell growth, proliferation and metastasis²⁰. Previous studies have reported that CD24 is overexpressed in nearly 70% of human cancers, and intracellular CD24 disrupts the ARF-NPM interaction and enables mutational and viral oncogene-mediated p53 inactivation²¹. CD24 is significantly correlated with tumorigenesis genes, such as non-coding RNAs²². It was previously demonstrated that a subpopulation of adipocyte progenitor cells was identified with the expression of the cell surface molecule CD24 being critically important for reconstitution of white adipose tissue function *in vivo*²³. CD24 was shown to be important in the reconstitution of white adipocyte (WAT) function *in vivo*, as well as a specific regulator of adipogenesis *in vitro*^{23,24}. Furthermore, it was demonstrated that losing CD24 in male mice leads to a generalized reduction of WAT and metabolic disturbances²⁴. Fairbridge *et al.*²⁵ reported that the global absence of CD24 affects adipocyte cell size *in vivo* in a sex- and diet-dependent manner, as well as causing metabolic disturbances in glucose homeostasis and free fatty acid levels. However, the precise function of CD24 and the underlying mechanisms of its activity in NAFLD/NASH progression remain unclear. This is the first study to identify the prominent correlation between CD24 and NAFLD/NASH.

Insulin resistance (IR) is central in the pathogenesis of NAFLD. NAFLD often significantly impacts glucose and lipid metabolism by exacerbating hepatic IR²⁶. CD24 can regulate lipid raft occupancy and may affect glucose uptake by regulating lipid raft protein localization²⁷. Additional studies will be required to identify whether there is a potential mechanism among CD24, glucose uptake, and insulin resistance. IR is a major factor for hepatic fat accumulation²⁸. Several studies only focused on a single protein, which ignored the various potential pathways in this complex disease²⁹. In our study, we found that “glycolysis/gluconeogenesis”, “p53 signaling pathway” and “glycine, serine and threonine metabolism” were 3 intersecting pathways in the relation network. Several studies have reported that glycolysis/gluconeogenesis³⁰, the p53 signaling pathway³¹, and glycine metabolism³² were each associated with IR. The biological process “small molecule metabolic process” was reported to be vital in cancer³³, hepatic metabolism disorder like IR³⁴. We supposed it to be a key biological process in fatty liver. Further studies will be required to determine whether the co-expressed DEGs including CD24 could activate one of these pathways or other mechanisms to induce NAFLD/NASH in humans.

In summary, we first used the GCBI bioinformatics analysis platform to identify DEGs between NAFLD/NASH tissues and normal liver tissues, which showed that CD24 is the hub gene and identify 3 intersecting pathways in the relation network. Then, using qRT-PCR analysis, we concluded that the mRNA expression of CD24 is upregulated in fatty liver. Further studies are required to elucidate the function and underlining mechanisms of this potential biomarker in the progression of hepatocyte steatosis.

References

- Williams, C. D. *et al.* Prevalence of nonalcoholic fatty liver disease and nonalcoholic steatohepatitis among a largely middle-aged population utilizing ultrasound and liver biopsy: a prospective study. *Gastroenterology* **140**, 124–131 (2011).
- Younossi, Z. M., Henry, L., Bush, H. & Mishra, A. Clinical and economic burden of nonalcoholic fatty liver disease and nonalcoholic steatohepatitis. *Clin. Liver Dis.* **22**, 1–10 (2018).
- Hardy, T., Oakley, F., Anstee, Q. M. & Day, C. P. Nonalcoholic fatty liver disease: pathogenesis and disease spectrum. *Annu. Rev. Pathol.* **11**, 451–496 (2016).
- Kim, G. A. *et al.* Association between non-alcoholic fatty liver disease and cancer incidence rate. *J. Hepatol.* **68**, 140–146 (2018).
- Wolf, M. J. *et al.* Metabolic activation of intrahepatic CD8+ T cells and NKT cells causes nonalcoholic steatohepatitis and liver cancer via cross-talk with hepatocytes. *Cancer Cell* **26**, 549–564 (2014).
- Cohen, J. C., Horton, J. D. & Hobbs, H. H. Human fatty liver disease: old questions and new insights. *Science* **332**, 1519–1523 (2011).
- Kim, W. R. *et al.* OPTN/SRTR 2015 annual data report: liver. *Am. J. Transplant.* **17**(Suppl 1), 174–251 (2017).
- Wree, A., Broderick, L., Canbay, A., Hoffman, H. M. & Feldstein, A. E. From NAFLD to NASH to cirrhosis-new insights into disease mechanisms. *Nat. Rev. Gastroenterol. Hepatol.* **10**, 627–636 (2013).
- Haas, J. T., Francque, S. & Staels, B. Pathophysiology and mechanisms of nonalcoholic fatty liver disease. *Annu. Rev. Physiol.* **78**, 181–205 (2016).
- Hanin, G. *et al.* miRNA-132 induces hepatic steatosis and hyperlipidaemia by synergistic multitarget suppression. *Gut*. <https://doi.org/10.1136/gutjnl-2016-312869> (2017).
- Moylan, C. A. *et al.* Hepatic gene expression profiles differentiate presymptomatic patients with mild versus severe nonalcoholic fatty liver disease. *Hepatology* **59**, 471–482 (2014).
- Murphy, S. K. *et al.* Relationship between methylome and transcriptome in patients with nonalcoholic fatty liver disease. *Gastroenterology* **145**, 1076–1087 (2013).
- Feng, A., Tu, Z. & Yin, B. The effect of HMGB1 on the clinicopathological and prognostic features of non-small cell lung cancer. *Oncotarget* **7**, 20507–20519 (2016).
- Li, O., Zheng, P. & Liu, Y. CD24 expression on T cells is required for optimal T cell proliferation in lymphopenic host. *J. Exp. Med.* **200**, 1083–1089 (2004).
- Deugnier, M. A. *et al.* Isolation of mouse mammary epithelial progenitor cells with basal characteristics from the Comma-Dbeta cell line. *Dev. Biol.* **293**, 414–425 (2006).
- Wang, X. *et al.* Nestin⁺CD24^{low} population from fetal nestin-EGFP transgenic mice enriches the pancreatic endocrine progenitor cells. *Pancreas* **31**, 385–391 (2005).
- Shakiba, N. *et al.* CD24 Tracks Divergent Pluripotent States in Mouse and Human Cells. *Nat Commun.* **6**, 7329 (2015).
- Kim, T. S., Gorski, S. A., Hahn, S., Murphy, K. M. & Braciale, T. J. Distinct Dendritic Cell Subsets Dictate the Fate Decision Between Effector and Memory CD8(+) T Cell Differentiation by a CD24-dependent Mechanism. *Immunity* **40**, 400–413 (2014).
- Turcan, S. *et al.* Mutant-IDH1-dependent Chromatin State Reprogramming, Reversibility, and Persistence. *Nat Genet.* **50**, 62–72 (2018).
- Lee, J. H., Kim, S. H., Lee, E. S. & Kim, Y. S. CD24 overexpression in cancer development and progression: a meta-analysis. *Oncol. Rep.* **22**, 1149–1156 (2009).
- Wang, L. *et al.* Intracellular CD24 disrupts the ARF-NPM interaction and enables mutational and viral oncogene-mediated p53 inactivation. *Nat. Commun.* **6**, 5909 (2015).
- Wang, X. *et al.* Long non-coding RNA DILC regulates liver cancer stem cells via IL-6/STAT3 axis. *J. Hepatol.* **64**, 1283–1294 (2016).

23. Rodeheffer, M. S., Birsoy, K. & Friedman, J. M. Identification of white adipocyte progenitor cells *in vivo*. *Cell* **135**, 240–249 (2008).
24. Smith, N. C., Fairbridge, N. A., Pallegar, N. K. & Christian, S. L. Dynamic upregulation of CD24 in pre-adipocytes promotes adipogenesis. *Adipocyte* **4**, 89–100 (2015).
25. Fairbridge, N. A. *et al.* Loss of CD24 in Mice Leads to Metabolic Dysfunctions and a Reduction in White Adipocyte Tissue. *Plos One*. **10**, e141966 (2015).
26. Liu, Q., Bengmark, S. & Qu, S. The role of hepatic fat accumulation in pathogenesis of non-alcoholic fatty liver disease (NAFLD). *Lipids Health Dis.* **9**, 42 (2010).
27. Runz, S. *et al.* CD24 induces localization of beta1 integrin to lipid raft domains. *Biochem. Biophys. Res. Commun.* **365**, 35–41 (2008).
28. Wang, X. C., Zhan, X. R., Li, X. Y., Yu, J. J. & Liu, X. M. Identification and validation co-differentially expressed genes with NAFLD and insulin resistance. *Endocrine* **48**, 143–151 (2015).
29. Lambert, J., Berger, T., Mak, T. W., van Helden, J. & Weiskirchen, R. Lipocalin-2 in fructose-induced fatty liver disease. *Front. Physiol.* **8**, 964 (2017).
30. Nagarajan, S. R. *et al.* Insulin and diet-induced changes in the ubiquitin-modified proteome of rat liver. *PLOS One* **12**, e0174431 (2017).
31. Zhang, X. *et al.* Overexpression of p53 improves blood glucose control in an insulin resistant diabetic mouse model. *Pancreas* **45**, 1010–1017 (2016).
32. Adeva-Andany, M. M., López-Maside, L., Donapetry-García, C., Fernández-Fernández, C. & Sixto-Leal, C. Enzymes involved in branched-chain amino acid metabolism in humans. *Amino Acids* **49**, 1005–1028 (2017).
33. Wang, H. *et al.* Biological Analysis of Cancer Specific microRNAs On Function Modeling in Osteosarcoma. *Sci Rep.* **7**, 5382 (2017).
34. Tian, X. *et al.* Transcriptome Analysis Reveals the Molecular Mechanism of Hepatic Metabolism Disorder Caused by Chromium Poisoning in Chickens. *Environ Sci Pollut Res Int.* (2018).

Acknowledgements

This study was supported by the National Natural Science Foundation of China (81373156, 81471583 and 81570587), Guangdong Provincial international Cooperation Base of Science and Technology (Organ Transplantation) (2015B050501002), Guangdong Provincial Natural Science Funds for Major Basic Science Culture Project (2015A030308010), Guangdong Provincial Natural Science Funds for Distinguished Young Scholars (2015A030306025), Special Support Program for Training High-level Talent in Guangdong Province (2015TQ01R168), Pearl River Nova Program of Guangzhou (201506010014), and the Science and Technology Program of Guangzhou (201704020150), the National Natural Science Foundation of China (grant 81670592), the Natural Science Foundation of Guangdong Province, China (grant 2016A030313242); the Medical Scientific Research Foundation of Guangdong Province, China (grant A2016033), the Science and Technology Program of Guangzhou, China (grant 201804020075), and the Fundamental Research Funds for the Central Universities (grant 17ykjc09), the Program Sci-tech Research Development of Guangdong Province (2014A020212717), and the Science and Technology Program of Huizhou (170520181743174).

Author Contributions

Conceived and designed the study: S.Z.H., C.J.S., Q.Z. and L.W.W.; Searched databases: Y.C.H., Y.H.T. and Z.B.Z.; Data analyses: Z.H.Z., Y.X.Z. and L.H.W.; Preparation of tables and figures: Q.Z., M.G.C., Z.Y.G., D.P.W. and W.Q.J.; Wrote and revised the manuscript: S.Z.H., C.J.S., L.W.W. and X.S.H.; All authors reviewed the manuscript.

Additional Information

Supplementary information accompanies this paper at <https://doi.org/10.1038/s41598-018-25658-4>.

Competing Interests: The authors declare no competing interests.

Publisher's note: Springer Nature remains neutral with regard to jurisdictional claims in published maps and institutional affiliations.



Open Access This article is licensed under a Creative Commons Attribution 4.0 International License, which permits use, sharing, adaptation, distribution and reproduction in any medium or format, as long as you give appropriate credit to the original author(s) and the source, provide a link to the Creative Commons license, and indicate if changes were made. The images or other third party material in this article are included in the article's Creative Commons license, unless indicated otherwise in a credit line to the material. If material is not included in the article's Creative Commons license and your intended use is not permitted by statutory regulation or exceeds the permitted use, you will need to obtain permission directly from the copyright holder. To view a copy of this license, visit <http://creativecommons.org/licenses/by/4.0/>.

© The Author(s) 2018